International Journal of Power Electronics and Drive Systems (IJPEDS)
Vol. 7, No. 3, September 2016, pp. 677 – 686
ISSN: 2088-8694

Backstepping Control of Wind and Photovoltaic Hybrid Renewable Energy System

Marouane El Azzaoui*, Hassane Mahmoudi*, and Karima Boudaraia*

*Electronics Power and Control Team, Department of Electrical Engineering, Mohammadia School of Engineers, Mohammed V University, Rabat, Morocco.

Article Info

Article history:

Received Jun 14, 2016
Revised Aug 19, 2016
Accepted Aug 30, 2016

Keyword:

Doubly fed induction generator
Wind turbine
Backstepping control
Lyapunov approach
PV system

ABSTRACT

This paper deals with the interconnected grid hybrid renewable energy system (HRES). The wind energy conversion system (WECS), is built around a wind turbine coupled to a doubly fed induction generator (DFIG). The stator of DFIG is directly related to the grid and the rotor is connected to the grid through back-to-back power converters. The proposed algorithm combines the nonlinear Backstepping approach and the field orientation applied to control the DFIG. In a first step, this technique is applied to the side converter rotor (RSC), to control the electromagnetic torque and reactive power, and secondly, it is applied to the grid side converter (GSC) to control the power exchanged with the grid and regulate the DC bus voltage. The PV energy system is composed by the PV array and the DC-DC boost converter which controlled by the MPPT method to extract the optimal power. Simulations results present the performances in terms of set point tracking, stability, and robustness with respect to the variation in wind speed and irradiation.

Copyright © 2016 Insitute of Advanced Engineeering and Science.
All rights reserved.

Corresponding Author:
Marouane El Azzaoui
Electronics Power and Control Team, Department of Electrical Engineering, Mohammadia School of Engineers, Mohammed V University, Rabat, Morocco.
E-mail: marouane.elazzaoui@research.emi.ac.ma

1. INTRODUCTION

Hybrid systems renewable energies (HRES) are became popular in the typologies of renewable energy. A HRES is composed of two or more renewable energy sources with appropriate energy conversion technology connected together to feed power to the local load or grid [1]. We are interested in this paper to combine wind and PV because they are the most promising technologies for supplying load in remote and rural regions. The most used generator in wind turbine is the DFIG due to its advantages in variable wind speed such as the low sizing of the back-to-back converter, and its stability on the hypo and hyper synchronous modes [2].

This paper presents a theoretical framework for a Backstepping control strategy of the doubly fed induction generator and related power equipments. This technique is a relatively new control method for nonlinear systems. It allows sequentially and systematically, to determine the system's control law, by the choice of a Lyapunov function. Its principle is to set up in a constructive manner the control law of the nonlinear system by considering some state variables as virtual drives and develop intermediate control laws [3]. The DC-DC boost converter is controlled by MPPT strategy to follows the maximum power point.

This paper is organized as follows: in Section 2, a brief description of the system studied is presented. In section 3, the modeling of the turbine, the DFIG, and the photovoltaic system is presented respectively. In the section 4, the control strategy of the hybrid wind/PV system is depicted, in which we propose a backstepping control for the RSC and GSC respectively. Then the MPPT PV subsystem is shown and the DC-bus voltage is exposed. The control performances are illustrated through numerical simulations in section 6.

2. PRESENTATION OF THE STUDIED SYSTEM

The basic configuration of the whole system is presented in figure (1). The studied system is formed by three bladed rotors with a corresponding mechanical gearbox, a DFIG, two power converters (RSC and GSC), a DC bus voltage, a PV generator, a DC-DC boost converter and a grid filter. The coupling of the two subsystems (wind and PV) is made via a DC-bus. GSC works as a rectifier and RSC works as an inverter when the machine is driven below synchronous speed. In this case the rotor of the DFIG receives the power from the grid. When the machine is driven above the synchronous speed, GSC works as an inverter and RSC works as a rectifier, in this case the rotor of the DFIG generates the power to the grid.

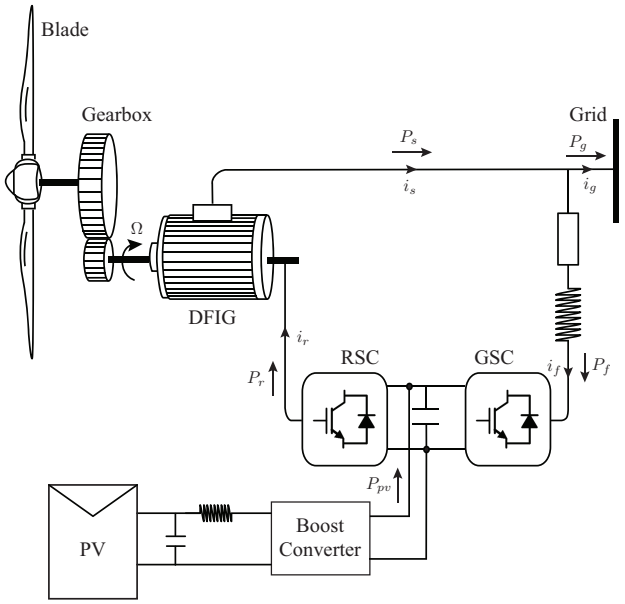

Figure 1. Wind energy conversion system

3. MODELING OF THE HYBRID WIND/PV SYSTEM COMPONENTS

3.1. Turbine modeling

The expression of aerodynamic power of the turbine is given by:

$$P_t = \frac{1}{2}.\rho.\pi.R^2.C_p(\lambda,\beta).v^3 \tag{1}$$

ρ is the air density, R is the blade radius, λ is the speed ratio, β is the pitch angle ,v is the wind speed, and C_p is the power coefficient

The expression of the torque is obtained by dividing the power by the torque speed.

$$T_t = \frac{1}{2\Omega_t}.\rho.\pi.R^2.C_p(\lambda,\beta).v^3 \tag{2}$$

Power coefficient is given as function of pitch angle and speed ratio, its expression in this work is expressed by the the following equation [4]:

$$C_p(\lambda,\beta) = A.\sin\left(\frac{\pi.(\lambda+0.1)}{14.34-0.3.(\beta-2)}\right) - B \tag{3}$$

with: $[A = 0.35 - 0.0167.(\beta-2)$ and $B = 0.00184.(\lambda-3)(\beta-2)$. The speed ratio λ is given by:

$$\lambda = \frac{R\Omega_t}{v} \tag{4}$$

Speeds and torques of the turbine and the generator are related respectively by:

$$T_t = GT_g \tag{5}$$

$$\Omega = G\Omega_t \tag{6}$$

The dynamics of the mechanical speed of the DFIG is obtained by applying the fundamental equation of dynamics:

$$J\frac{d\Omega}{dt} = Tg - f\Omega - T_{em} \tag{7}$$

Where: T_{em} is the electromagnetic torque, J is the total inertia, and f is the friction coefficient.
Figure (2) shows the block diagram of the turbine obtained by the above equations.

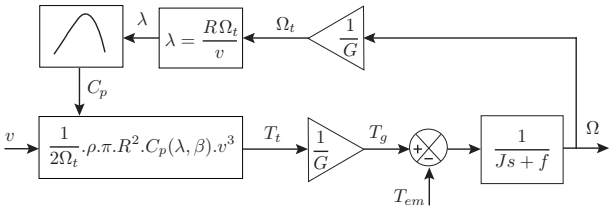

Figure 2. Block diagram of the turbine

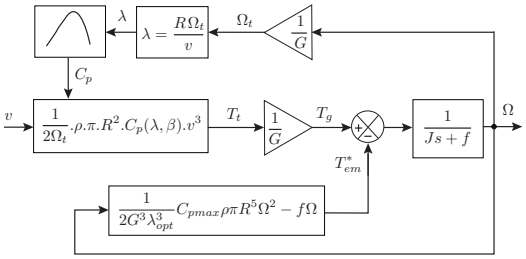

Figure 3. Block diagram of wind turbine MPPT

3.2. Wind turbine Maximum power extraction

In this section, a MPPT technique without sensing the wind speed is presented. The strategy proposed assumes that the wind speed varies a little in permanent regime. Under this consideration the mechanical equation is described by [5]:

$$J\frac{d\Omega_m}{dt} = 0 = T_{mec} = T_{fa} - T_{em} - f\Omega \tag{8}$$

Electromagnetic torque expression becomes:

$$T^*_{em} = \frac{1}{2G\Omega_t} C_{pmax}\rho S v^3 - f\Omega \tag{9}$$

in this work the pitch angle β is maintained constant. Equation (4) allows to estimate the wind speed as follows:

$$v = \frac{R\Omega_t}{\lambda_{opt}} \tag{10}$$

Substituting Equation (10) in (9) The electromagnetic torque reference becomes:

$$T^*_{em} = \frac{1}{2G^3\lambda^3_{opt}} C_{pmax}\rho\pi R^5\Omega^2 - f\Omega \tag{11}$$

The block diagram of the MPPT without sensing the wind speed is shown in figure (3).

3.3. DFIG modeling

Stator and rotor voltages of the DFIG in d-q frame reference is written as follows [6]:

$$\begin{cases} V_{sd} = R_s I_{sd} + \dfrac{d\varphi_{sd}}{dt} - \omega_s\varphi_{sq} \\ V_{sq} = R_s I_{sq} + \dfrac{d\varphi_{sq}}{dt} + \omega_s\varphi_{sd} \\ V_{rd} = R_r I_{rd} + \dfrac{d\varphi_{rd}}{dt} - \omega_r\varphi_{rq} \\ V_{rq} = R_r I_{rq} + \dfrac{d\varphi_{rq}}{dt} + \omega_r\varphi_{rd} \end{cases} \tag{12}$$

Stator and rotor flux are expressed by:

$$\begin{cases} \varphi_{sd} = L_s I_{sd} + L_m I_{rd} \\ \varphi_{sq} = L_s I_{sq} + L_m I_{rq} \\ \varphi_{rd} = L_r I_{rd} + L_m I_{sd} \\ \varphi_{rq} = L_r I_{rq} + L_m I_{sq} \end{cases} \tag{13}$$

Stator, rotor, and mechanical speed are linked by the following equation:

$$\omega_r = \omega_s - p\Omega \tag{14}$$

Stator and rotor expressions of the active and reactive powers are given by:

$$\begin{cases} P_s = V_{sd} I_{sd} + V_{sq} I_{sq} \\ Q_s = V_{sq} I_{sd} + V_{sd} I_{sq} \\ P_r = V_{rd} I_{rd} + V_{rq} I_{rq} \\ P_r = V_{rq} I_{rd} + V_{rd} I_{rq} \end{cases} \tag{15}$$

The electromagnetic torque is given by:

$$T_{em} = \frac{pL_m}{L_s}(\varphi_{sq} I_{rd} - \varphi_{sd} I_{rq}) \tag{16}$$

We consider the assumption that the stator resistance is neglected. This assumption is verified for the medium and high power machines used in wind turbines [7]. Under stator field orientation control, stator voltage becomes:

$$\begin{cases} V_{ds} = 0 \\ V_{qs} = V_s = \omega_s \varphi_{sd} \end{cases} \tag{17}$$

The expressions of the active and reactive power equations become:

$$\begin{cases} P_s = -V_s \dfrac{L_m}{L_s} I_{rq} \\ Q_s = -Vs \dfrac{Lm}{Ls} I_{rd} + \dfrac{V_s^2}{\omega_s Ls} \end{cases} \tag{18}$$

The electromagnetic torque becomes:

$$T_{em} = -\frac{pLmVs}{\omega_s L_s} I_{rq} \tag{19}$$

Hence, rotor currents as function of the rotor voltages is given by:

$$\begin{cases} \dfrac{dI_{rd}}{dt} = \dfrac{1}{\sigma Lr}(V_{rd} - RrI_{rd} + \sigma Lr\omega_r I_{rq}) \\ \dfrac{dI_{rq}}{dt} = \dfrac{1}{\sigma Lr}(V_{rd} - RrI_{rq} - \sigma Lr\omega_r I_{rd} - g\dfrac{L_m V_s}{L_s}) \end{cases} \tag{20}$$

3.4. Photovoltaic system modeling

The phenomenenon named photovoltaic effect consists mainly transforming the solar light in electric energy by means of the semi conductor devices named photovoltaic cells. Figure (4) shows the equivalent circuit diagram of a single solar cell. Here I_{ph} is the photo current source with a reverse connected diode. R_s and R_{sh} are series and shunt resistances respectively.

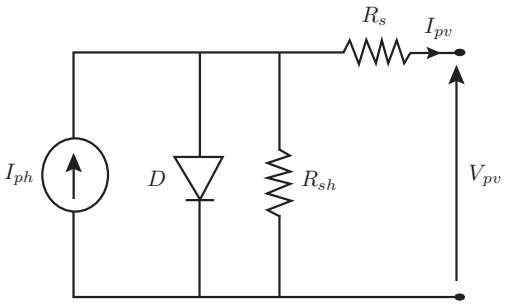

Figure 4. Electric model of a photovoltaic cell

The output current from the photovoltaic array is:

$$I_{pv} = I_{ph} - I_d \tag{21}$$

The direct current diode is writing as follows:

$$I_d = I_s \left[\exp\left(\frac{qV_d}{KT}\right) - 1 \right] \tag{22}$$

Where I_s is the reverse saturation current of the diode, q is the electron charge, V_d is the voltage across the diode,K is Boltzmann constant $1.38\,10^{-19} J/K$ and T is the junction temperature in Kelvin (k). Substituting (22) in (21) gives:

$$I_{pv} = I_{ph} - I_s \left[\exp\left(\frac{qV_d}{KT}\right) - 1 \right] \tag{23}$$

The voltage across diode writes as:

$$V_d = \frac{V_{pv} - I_{pv} R_s}{N} \tag{24}$$

Substituting (24) in (23) gives:

$$I_{pv} = I_{ph} - I_s \left[\exp\left(\frac{q(V_{pv} - I_{pv} R_s)}{NKT}\right) - 1 \right] \tag{25}$$

Where, V_{pv} is the PV cell voltage and N is the diode ideality factor.

4. HYBRID WIND/PV SYSTEM CONTROL STRATEGY

Each of the two energy sources (Wind and PV) is controlled so as to deliver energy at optimum efficiency. The adaptive Backstepping control is employed to achieve maximum power tracking for a DFIG driven by a wind turbine and PV to deliver this MPPT to regulate the output voltage.

4.1. Backstepping control of RSC

The basic idea of the Backstepping design is the use of the so-called virtual control to systematically decompose a complex nonlinear control design problem into simpler, smaller ones. Roughly speaking, Backstepping design is divided into various design steps [8, 9]. In each step we essentially deal with an easier, single-input-single-output design problem, and each step provides a reference for the next design step. The overall stability and performance are achieved by a Lyapunov function for the whole system. The synthesis of this control can be achieved in two steps [10].

4.1.1. Step 1: calculation of the rotor currents

Let's define e_1 the error between the actual reference toques, and e_2 the error between the stator reactive power and its reference.

$$\begin{cases} e_1 = T_{em}^* - T_{em} \\ e_2 = Q_s^* - Q_s \end{cases} \tag{26}$$

The derivative of errors are calculated as:

$$\begin{cases} \dot{e}_1 = \dot{T}^*_{em} + \dfrac{pLmV_s}{\omega_s L_s}\dot{I}_{rq} \\ \dot{e}_2 = \dot{Q}^*_s + \dfrac{L_m V_s}{L_s}\dot{I}_{rd} \end{cases} \tag{27}$$

The first Lyapunov function is defined as:

$$V_1 = \frac{1}{2}e_1^2 + \frac{1}{2}e_2^2 \tag{28}$$

Its derivative is:

$$\dot{V}_1 = e_1\dot{e}_1 + e_2\dot{e}_2 \tag{29}$$

Substituting (27) into (29), we get:

$$\dot{V}_1 = e_1\left[\dot{T}^*_{em} + \frac{pL_mV_s}{\sigma L_r L_s\omega_s}\left(V_{rq} - R_rI_{rq} - \omega_r I_{rd} - g\frac{L_mV_s}{L_s}\right)\right] + e_2\left[\dot{Q}^*_s + \frac{L_mV_s}{\sigma L_rL_s}\left(V_{rd} - R_rI_{rd} + \omega_r I_{rq}\right)\right] \tag{30}$$

To track references values of the torque and reactive power, references rotor currents are calculated as follows:

$$\begin{cases} I^*_{rq} = A_1[k_1e_1 + T^*_{em} + A_2(V_{rq} - \sigma L_r\omega_r I_{rd} - g\dfrac{L_mV_s}{L_s})] \\ I^*_{rd} = B_1\left[k_2e_2 + Q^*_s + B_2(V_{rd} + \sigma L_r\omega_r I_{rq})\right] \end{cases} \tag{31}$$

With :

$$A_1 = \frac{\sigma L_rL_s\omega_s}{pL_mV_sR_r} \qquad A_2 = \frac{\sigma L_rpL_mV_s}{\omega_sL_s} \qquad B_1 = \frac{\sigma L_rL_s}{L_mV_sR_r} \qquad B_2 = \frac{\sigma L_rL_s}{L_mV_s}$$

where k_1 and k_2 are positive constants. The derivative of the Lyapunov function is negative:

$$\dot{V}_1 = -k_1e_1^2 - k_2e_2^2 < 0 \tag{32}$$

4.1.2. Step 2: calculation of the rotor voltages

In this step, the rotor currents errors, are defined by:

$$\begin{cases} e_3 = I^*_{rq} - I_{rq} \\ e_4 = I^*_{rd} - I_{rd} \end{cases} \tag{33}$$

Their derivatives are:

$$\begin{cases} \dot{e}_3 = \dot{I}^*_{rq} - \dfrac{1}{\sigma L_r}V_{rq} + C_1 \\ \dot{e}_4 = \dot{I}^*_{rd} - \dfrac{1}{\sigma L_r}V_{rd} + C_2 \end{cases} \tag{34}$$

with:

$$C_1 = \frac{1}{\sigma l_r}\left(R_rI_{rq} + \sigma L_r\omega_rI_{rd} + g\frac{L_mV_s}{L_s}\right)$$

$$C_2 = \frac{1}{\sigma l_r}\left(R_rI_{rd} - \sigma L_r\omega_rI_{rq}\right)$$

Final Lyapunov function is defined by the following equation:

$$V_2 = \frac{1}{2}(e_1^2 + e_2^2 + e_3^2 + e_4^2) \tag{35}$$

its derivative is:

$$\dot{V}_2 = e_1\dot{e}_1 + e_2\dot{e}_2 + e_3\dot{e}_3 + e_4\dot{e}_4 \tag{36}$$

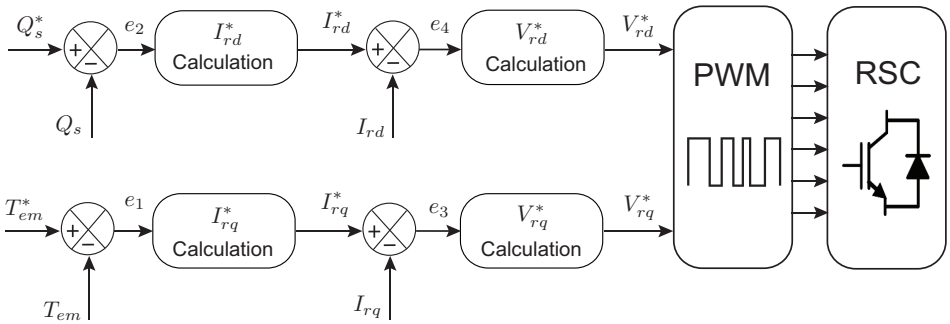

Figure 5. Block diagram of backstepping control of the RSC

By Substituting all errors expressions, we get the next expression of the lyapunov function:

$$\dot{V}_2 = -k_1 e_1^2 - k_2 e_2^2 - k_3 e_3^2 - k_4 e_4^2 + e_3(k_3 e_3 + \dot{I}_{rq}^* - \frac{1}{\sigma L_r} V_{rq} + C_1) + e_4(k_4 e_4 + \dot{I}_{rd}^* - \frac{1}{\sigma L_r} V_{rd} + C_2) \quad (37)$$

Therefore, the rotor voltages are given by:

$$\begin{cases} V_{rq}^* = \sigma L_r(k_3 e_3 + \dot{I}_{rq}^* + C_1) \\ V_{rd}^* = \sigma L_r(k_4 e_4 + \dot{I}_{rd}^* + C_2) \end{cases} \quad (38)$$

Where k_3 and k_4 are positive constants.
So, the lyapunov function is negative as shown in the next equation:

$$\dot{V}_2 = -k_1 e_1^2 - k_1 e_2^2 - k_3 e_3^2 - k_4 e_4^2 < 0 \quad (39)$$

Block diagram of the RSC control is presented in figure (5).

4.2. Backstepping Control of Grid side converter

The currents crossing the RL filter, are expressed in d-q frame reference by:

$$\begin{cases} \frac{dI_{fd}}{dt} = -\frac{V_{fd}}{L_f} - \frac{R_f}{Lf} I_{fd} + \omega_s I_{fq} \\ \frac{dI_{fq}}{dt} = -\frac{V_{fq}}{L_f} - \frac{R_f}{Lf} I_{fq} - \omega_s I_{fd} + \frac{V_{sq}}{L_f} \end{cases} \quad (40)$$

Considering the stator field orientation ($V_{sd} = 0$). The powers provided by GSC are given by:

$$\begin{cases} P_f = V_{sq} I_{fq} \\ Q_f = -V_{sq} I_{fd} \end{cases} \quad (41)$$

The control of powers is obtained by controlling the currents, this is why errors e_1 and e_2 are the difference between the desired and actual d-q currents:

$$\begin{cases} e_1 = (I_{fd})_d - I_{fd} \\ e_2 = (I_{fq})_d - I_{fq} \end{cases} \quad (42)$$

Their derivatives are:

$$\begin{cases} \dot{e}_1 = (\dot{I}_{fd})_d + \frac{V_{fd}}{L_f} + \frac{R_f}{Lf} I_{fd} - \omega_s I_{fq} \\ \dot{e}_2 = (\dot{I}_{fq})_d + \frac{V_{fq}}{L_f} + \frac{R_f}{Lf} I_{fq} + \omega_s I_{fd} - \frac{V_{sq}}{L_f} \end{cases} \quad (43)$$

The lyapunov function is chosen as:

$$V = \frac{1}{2}(e_1^2 + e_2^2) \quad (44)$$

Its derivative is:

$$\dot{V} = e_1\dot{e_1} + e_2\dot{e_2} \tag{45}$$

Replacing the terms of errors, we get:

$$\dot{V} = e_1\left[(\dot{I}_{fd})_d + \frac{V_{fd}}{L_f} + \frac{R_f}{Lf}I_{fd} - \omega_s I_{fq}\right] + e_2\left[(\dot{I}_{fq})_d + \frac{V_{fq}}{L_f} + \frac{R_f}{Lf}I_{fq} + \omega_s I_{fd} - \frac{V_{sq}}{L_f}\right] \tag{46}$$

Finnaly, the control voltages is given by:

$$\begin{cases} V_{fd} = -L_f\left[(\dot{I}_{fd})_d + \dfrac{R_f}{Lf}I_{fd} - \omega_s I_{fq} + k_1 e_1\right] \\ V_{fq} = -L_f\left[(\dot{I}_{fq})_d + \dfrac{R_f}{Lf}I_{fq} + \omega_s I_{fd} - \dfrac{V_{sq}}{L_f} + k_2 e_2\right] \end{cases} \tag{47}$$

Where k_1 and k_2 are positive constants.
Block diagram of the RSC control is presented in figure (6).

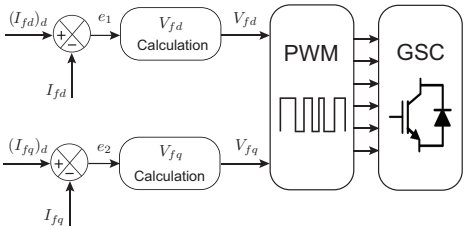

Figure 6. Backstepping control of the GSC

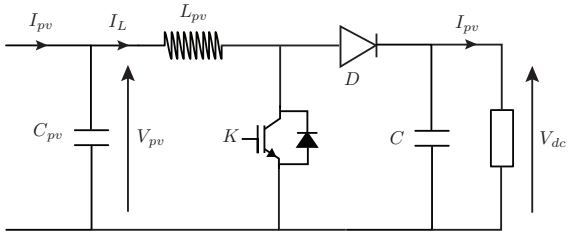

Figure 7. Circuit Diagram of boost converter

4.3. Control of PV subsystem

In a DC-DC Boost converter, the average output voltage V_{out} is greater than the input voltage V_{in} [11]. Boost Converter mainly consists of one inductor and two switches (usually a transistor switch and a diode) as shown in figure (7).
The output voltage of boost converter is given by:

$$V_{out} = \frac{V_{in}}{1 - D} \tag{48}$$

While D is the duty cycle.

The commonly used control technique of the PV subsystem is the MPPT method that acting on the duty cycle automatically of the boost converter to bring the PV at its optimum operating value whatever the weather instability or sudden variations in loads that can occur at any time as presented in the figure.9. The classical MPPT technique is the P&O algorithm which consists of creating a perturbation by decreasing or increasing the duty cycle of the boost converter and then observing the direction of power change in the PV output. If the PV power increases, the direction of perturbation is maintained. Otherwise, it is reversed to resume convergence towards the new maximum power point.The flow chart of the P&O algorithm is shown in Figure (8).

4.4. DC bus voltage control

By neglecting the converter losses, In subsynchronous mode the flow of powers is written as [12]:

$$P_f = P_c + P_r - P_{pv} \tag{49}$$

Where $P_c = V_{dc}i_c$ is the power in the DC bus.

By adjusting the power P_f , it is possible to control the power P_c in the capacitor and therefore to regulate the DC bus voltage (Figure 10).

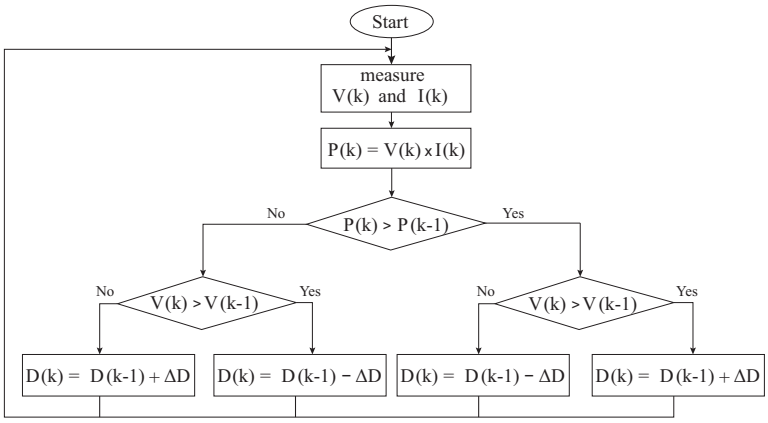

Figure 8. Flow chart of Perturb and observe algorithm

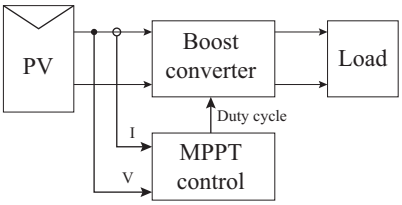

Figure 9. MPPT control of PV

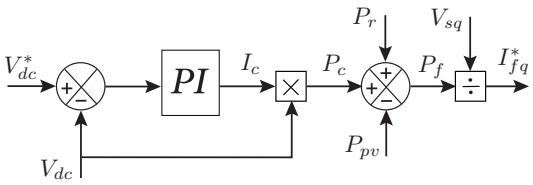

Figure 10. Control loop of the DC bus voltage

5. SIMULATIONS RESULTS

Simulations are made using Matlab/Simulink. In the following, we present the results for variable speed which is illustrated in figure (11a) representing subsynchronous and hypersynchronous modes, with irradiance 1000 W/m^2 and temperature 298 K.

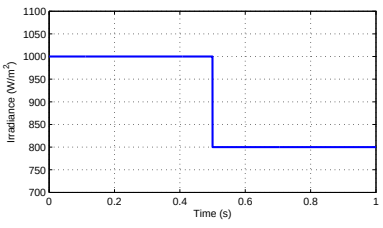

(a) Irradiance variation

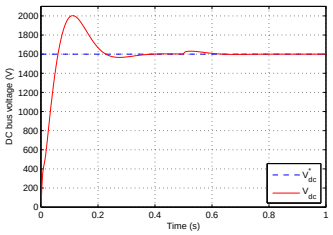

(b) DC bus voltage

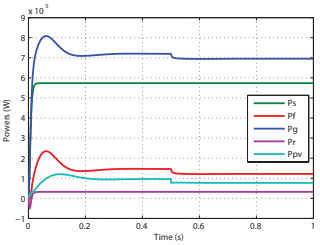

(c) HRES powers

Figure 12. Simulation results for HRES for constant wind speed (12.5 m/s) and variable irradiance

Figure (11b) shows that the reference DC bus voltage of hybrid system. This justifies the efficiency and the reliability of the DC bus control loop in tracking the predicted references. Figure (11c) shows that 25% of the power injected to the grid passes by the power converter. As well the grid power P_g is equal to the sum of the stator power P_s, the rotor power P_r, and the PV power P_{pv}.

Figure (12) shows the simulation results for a constant wind speed and variable irradiance. As shown by figure (12b), the DC bus voltage is well regulated. Figure (12c) illustrates the variations of the PV, wind and hybrid powers during the seek of the new maximum power point. For a constant wind speed and variable irradiance the system produces the maximum power ($P_s + P_r + P_{pv} = P_g$). The power supplied to the grid is the sum of wind and photovoltaic sources.

6. CONCLUSION

This paper examines a wind/PV hybrid energy system. The first subsystem consists of a wind system based DFIG, and the second consists of a photovoltaic generator PV.

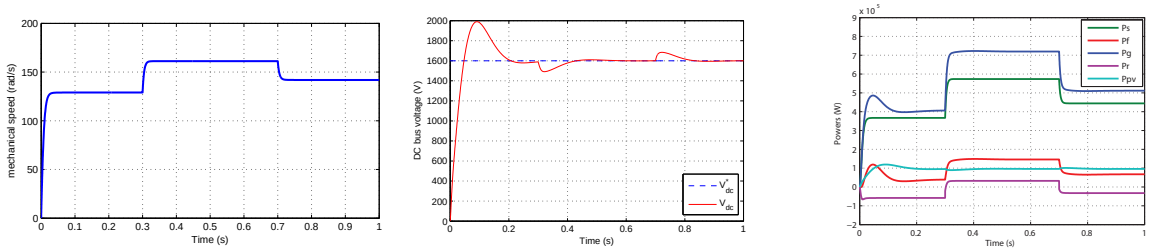

(a) Rotor speed (b) DC bus voltage (c) HRES powers

Figure 11. Simulation results for HRES for variable wind speed and constant irradiance

The wind energy system comprises two converters connected by a DC bus voltage allowing the exchange of power flowing between the grid and the machine. We used the non linear backstepping technique to control the RSC and GSC converters. The DC bus collects the energy generated by the two subsystems. The DC-DC boost converter is integrated with a PV generator and used to transfer the produced power to the grid through GSC. A MPPT strategy is used to extract the maximum power of the PV by adjusting the duty cycle of the boost converter.

Simulation results using Matlab/Simulink present the robustness against wind speed and irradiance variations.

REFERENCES

[1] G.Notton , M. Louche, "Autonomous hybrid photovoltaic power plant using a back-up generator: a case study," *Mediterranean Island. Renew Energy*,pp. 371–91, 1996.

[2] S. Khojet El Khil, I. Slama-Belkhodja, M. Pietrzak-David and B. De Fornel, "Power distribution law in a Doubly Fed Induction Machine," *Mathematics and Computers in Simulation*, volume 71, pages 360–368, 2006.

[3] A. Elmansouri, J. El mhamdi and A. Boualouch, "Control by Back Stepping of the DFIG Used in the Wind Turbine," *International Journal of Emerging Technology and Advanced Engineering*,Volume 5, Issue 2, February 2015.

[4] S. El Aimani, B. François, F. Minne et B. Robyns, "Comparison analysis of control structures for variable wind speed turbine," *Proceedings of CESA*, Lille, France, Juillet 2003.

[5] M. El Azzaoui, H. Mahmoudi, "Modeling and control of a doubly fed induction generator base wind turbine system optimizition of the power," *Journal of Theoretical and Applied Information Technology*, Vol 80, No 2, pp 304-314 October 2015.

[6] O.E. Elbashir, W. Zezhong, L. Qihui, "Analysis of DFIG Wind Turbine During Steady-State and Transient Operation," *TELKOMNIKA Indonesian Journal of Electrical Engineering*, Vol.12, No.6, June 2014, pp. 4148-4156.

[7] L. Zhang, C. Watthansarn and W. Shehered, "A matrix converter excited doubly-fed induction machine as a wind power generator," *IEEE Trans.Power Electronics and Variable Speed Drives*, vol. 2 ,pp 532–537, august 2002.

[8] M.R Jovanovic, B. Bamieh, "Architecture Induced by Distributed Backstepping Design," *IEEE Transactions on Automatic Control*, Vol.52, Issue. 1, pp. 108-113, January 2007.

[9] M. Moutchou, A. Abbou, H. Mahmoudi, "MRAS-based sensorless speed backstepping control for induction machine, using a flux sliding mode observeer," *Turkish Journal of Electrical Engineering and Computer Sciences*, 23: 187-200, 2015.

[10] M. El Azzaoui, H. Mahmoudi and C. Ed-dahmani, "Backstepping control of a Doubly Fed Induction Generator integrated to wind power system," *2016 International Conference on Electrical and Information Technologies (ICEIT)*, Tangiers, 2016, pp. 306-311.

[11] S.D. Stallon, K.V Kumar, S.S Kumar, "High Efficient Module of Boost Converter in PV Module," *International Journal of Electrical and Computer Engineering (IJECE)* , Vol.2, No.6, December 2012, pp. 758-781.

[12] Jerbi L., Krichen L. and Ouali A, "A fuzzy logic supervisor for active and reactive power control of a variable speed wind energy conversion system associated to a flywheel storage system," *Electric Power Systems Research*, Vol. 79, No 6, pp. 919–925, 2009.